JACS
JOURNAL OF THE AMERICAN CHEMICAL SOCIETY
Article
pubs.acs.org/JACS

Combination of Integrin-Binding Peptide and Growth Factor Promotes Cell Adhesion on Electron-Beam-Fabricated Patterns

Christopher M. Kolodziej,[†] Sung Hye Kim,[†] Rebecca M. Broyer,[†,‡] Sina S. Saxer,[†] Caitlin G. Decker,[†] and Heather D. Maynard*,[†]

[†]Department of Chemistry and Biochemistry and the California NanoSystems Institute, University of California, Los Angeles, 607 Charles E. Young Drive South, Los Angeles, California 90095, United States

Supporting Information

ABSTRACT: Understanding and controlling cell adhesion on engineered scaffolds is important in biomaterials and tissue engineering. In this report we used an electron-beam (e-beam) lithography technique to fabricate patterns of a cell adhesive integrin ligand combined with a growth factor. Specifically, micron-sized poly(ethylene glycol) (PEG) hydrogels with aminooxy- and styrene sulfonate-functional groups were fabricated. Cell adhesion moieties were introduced using a ketone-functionalized arginine-glycine-aspartic acid (RGD) peptide to modify the *O*-hydroxylamines by oxime bond formation. Basic fibroblast growth factor (bFGF) was immobilized by electrostatic interaction with the sulfonate groups. Human umbilical vein endothelial cells (HUVECs) formed focal adhesion complexes on RGD- and RGD and bFGF-immobilized patterns as shown by immunostaining of vinculin and actin. In the presence of both bFGF and RGD, cell areas were larger. The data demonstrate confinement of cellular focal adhesions to chemically and physically well-controlled microenvironments created by a combination of e-beam lithography and "click" chemistry techniques. The results also suggest positive implications for addition of growth factors into adhesive patterns for cell-material interactions.

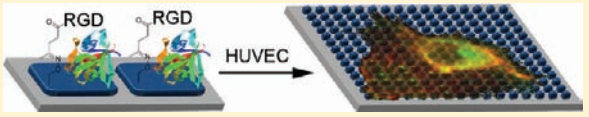

INTRODUCTION

The ability to create artificial surfaces capable of controlling cell adhesion is an important challenge in biomaterials, tissue engineering, and for biosensors.[1−3] In natural tissues, cells adhere to an extracellular matrix (ECM) composed mainly of fibronectin and proteoglycans, particularly heparan sulfate, supported on a collagen matrix. The ECM not only provides the physical microenvironment for cells, but also stores and mediates communication of numerous signaling molecules, which are essential for cell survival; these include growth factors, hormones, and cytokines.[4] Engineering an artificial surface that presents multiple components is therefore of great interest.

Integrins, which are heterodimeric transmembrane receptors, are responsible for cell adhesion and remodeling of the ECM.[5] They play important roles in embryonic development and growth, wound healing, angiogenesis, and inflammation.[6,7] Among the twenty-four known integrins, many bind specifically to the RGD sequence, which is the cell adhesion epitope of ECM proteins such as vitronectin and fibronectin.[8,9] RGD binds to the $\alpha_V\beta_3$ integrin found in endothelial cells, modulating angiogenesis and neovascularization.[10,11] RGD is also involved in osteoclast-mediated bone resorption[12,13] and metastasis.[14] Thus, RGD has widely been exploited on biomaterial surfaces.

bFGF is a universal signaling molecule that is found in the ECM, regulating numerous cell survival, differentiation, and tissue repair processes.[15] bFGF has been found to induce phosphorylation of Ser-910 on focal adhesion kinase (FAK), a part of the focal adhesion signaling pathway.[16] Heparan sulfate is an ECM component that acts as a depot for bFGF, and protects it from denaturation *in vivo*.[17−19] This is important because bFGF is easily inactivated. Therefore, heparinized, or heparin-mimetic materials have been widely exploited during implementation of bFGF to stabilize the growth factor.

There is significant potential for enhancing interactions between cells and biomaterials through cooperative binding. It has been demonstrated that growth factors coordinate integrin signaling.[6,20] Treatment with bFGF also improves the expression of $\alpha_V\beta_3$,[21] enhancing cell adhesion, motility, and proliferation.[22] Integrins and growth factor receptors share signaling pathways within the focal adhesion complex,[23] thus materials that activate both receptors can provide enhanced binding through synergistic effects.[24,25] Despite this potential, to our knowledge, there has only been one previous report of subcellular patterns of two signaling molecules with well-defined and -controlled dimensions, and this did not include bFGF.[26] Sorribas et al. demonstrated control over neurite outgrowth on 5 μm wide lines generated by a lift-off method and functionalized with RGD and axonin-1. Herein, we describe for the first time immobilization of both bFGF and RGD on patterned substrates.

One class of surfaces that offers control over the spatial arrangement of cell adhesion ligands are self-assembled monolayers (SAMs).[27] The suitability of SAMs as substrates for cell culture was first demonstrated by Massia and Hubbell using siloxane SAMs to immobilize RGD on glass substrates.[28]

Received: June 21, 2011
Published: November 29, 2011

Scheme 1. E-Beam Patterning of Silicon Substrates and Cell Adhesion[a]

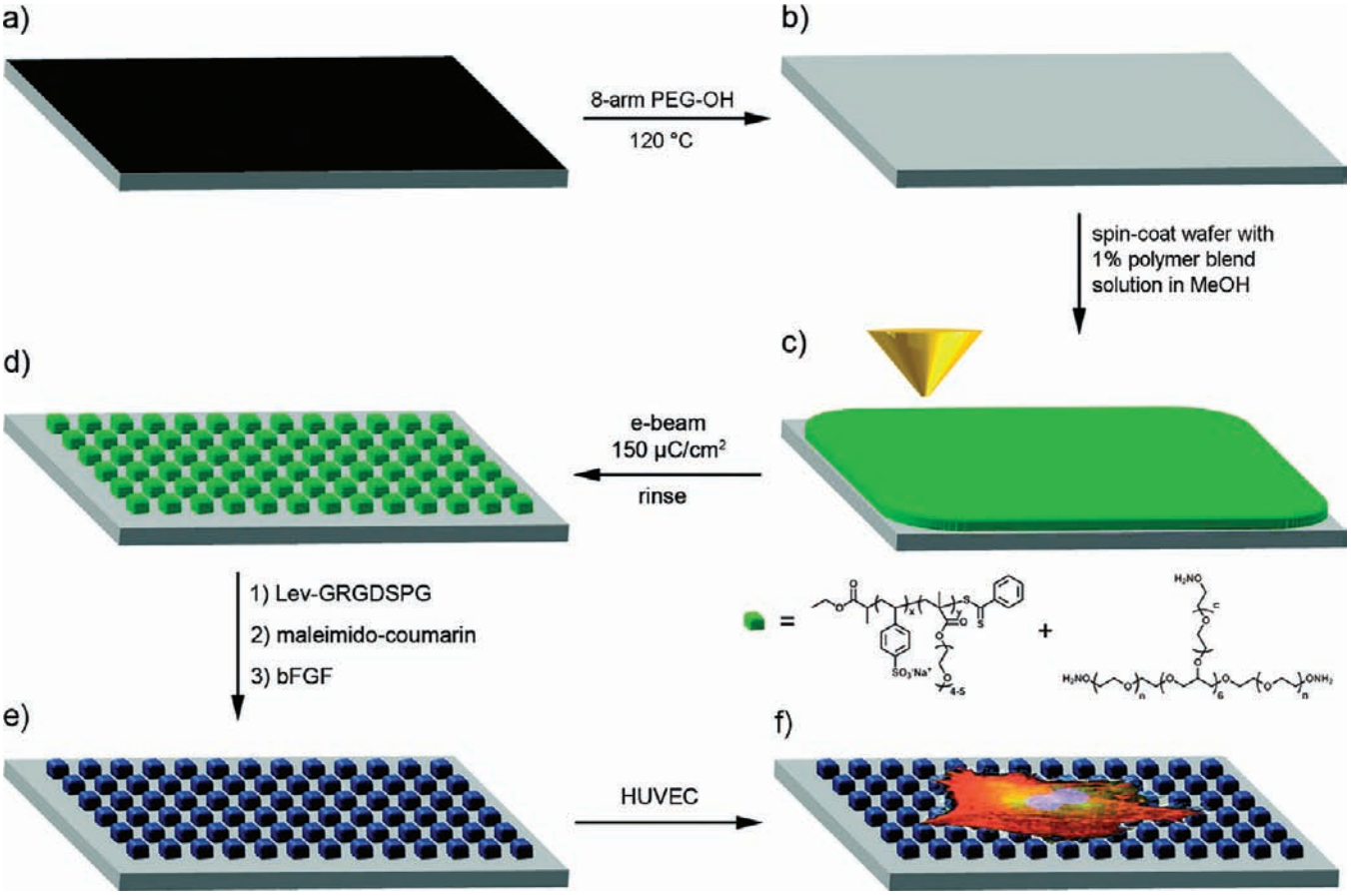

[a](a) Silicon wafers were spin-coated with 8-arm PEG-OH. (b) The 8-arm PEG-OH was then thermally annealed to the native oxide to passivate the surface. (c) Wafers spin-coated with 0.5% PEG-AO and 0.5% pSS-*co*-PEGMA were patterned by e-beam lithography. (d) The wafers were then rinsed to leave micropatterned hydrogels containing aminooxy and sulfonate functionality. (e) The wafers were then incubated with Lev-GRGDSPG, maleimido-coumarin, and finally bFGF to afford cell-adherent substrates. (f) HUVECs were then plated on the wafers, and cultured for 4 days.

A similar demonstration was made by Roberts and co-workers using thiol-on-gold SAMs of an RGD-bearing alkanethiol.[29] Several methods have been successfully developed to pattern these and similar SAMs to prepare surfaces for cell adhesion studies, including microcontact printing,[30−32] photolithography,[33,34] electron-beam (e-beam) lithography,[35] and dip-pen lithography.[36,37] These studies have demonstrated the importance of the spatial distribution of RGD for controlling cell survival,[30] migration,[33,37] and differentiation.[31] Block-copolymer micelle nanolithography, by Spatz and co-workers, allows for the formation of arrays of ECM components immobilized on gold nanoparticles with defined nanoscale spacing, and was used to determine a critical interspacing for focal adhesion formation.[38] Hierarchical patterning was also demonstrated by combining this technique with e-beam lithography.[39] However, because SAMs are susceptible to desorption, thiol exchange, lateral diffusion, and oxidation of thiols,[40,41] there is interest in the community for alternative fabrication strategies.

E-beam lithographic patterning of functionalized PEG is one technique that provides strong covalent attachment for potential long-term patterning. In addition, nanometer to micron-sized features are easily patterned. Upon exposure to electron-beam radiation, PEG cross-links to itself and to the underlying substrate via a radical mechanism.[42,43] This process forms hydrogels at the sites of exposure that are covalently immobilized on the surface and robust. The use of e-beam lithography for patterning PEG hydrogels was first reported by Krsko et al.,[44] and has been used by both Libera and our group to pattern biomolecules at the micro- and nanoscale.[45−50] These PEG hydrogels can be fabricated on plasma-generated silicon oxide,[44] on the native oxide of silicon,[49] or on a PEG-silane monolayer.[45] Furthermore, we recently showed that through the use of orthogonal chemistries it is possible to pattern multiple biomolecules in a single array with nanometer precision.[49] Krsko and co-workers have demonstrated that unfunctionalized PEG hydrogels patterned by e-beam lithography can direct the growth of neural cells.[51] However, to our knowledge e-beam lithography has not been used to fabricate surfaces that mimic the ECM through specific interactions with membrane receptors.

Herein, we describe use of e-beam lithography to prepare surfaces for controlled cell adhesion *via* presentation of dual ECM components. In this report, patterns were fabricated with well-defined spatial distribution incorporating RGD for cell adhesion and bFGF as a signalling molecule (Scheme 1). Poly(styrene-4-sulfonate-*co*-poly(ethylene glycol) methacrylate) (pSS-*co*-PEGMA) and 8-arm aminooxy-terminated PEG (PEG-AO) hydrogels were cross-linked on passivated silicon wafers. This surface was used to immobilize a ketone-functionalized RGD *via* oxime bond formation and bFGF *via* electrostatic interactions. Cell adhesion on the micropatterned

dx.doi.org/10.1021/ja205524x | *J. Am. Chem.Soc.* 2012, 134, 247−255

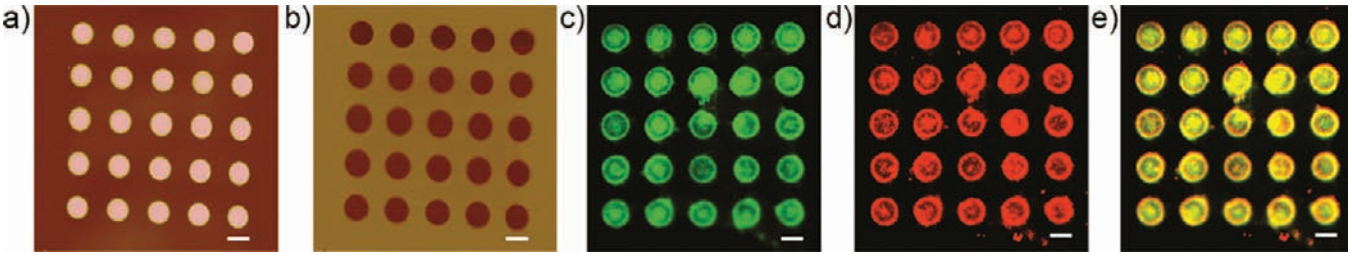

Figure 1. AFM and fluorescence images of RGD and bFGF immunostaining of test wafers. AFM images in both height (a) and phase (b) modes show uniform features, indicating that the two polymers patterned did not form phase-segregated domains. Fluorescence images of the patterns following immunostaining with integrin, antiintegrin mouse IgG, and AlexaFluor 488 antimouse IgG for RGD (c), and anti-FGF sheep IgG and AlexaFluor 568 antisheep IgG for bFGF (d) confirm the immobilization of the biomolecules on the patterns. (e) Colocalization of the two ECM components is observed in the composite image. Scale bars = 5 μm.

surfaces was investigated with HUVECs. Focal adhesion formation was verified and cell area was determined.

RESULTS AND DISCUSSION

In order to fabricate substrates capable of facilitating cell adhesion by mimicking the natural ECM, we designed surfaces, which include both RGD and bFGF or RGD alone. In order to ensure that nonspecific protein adsorption and cellular remodeling did not occur, the surfaces were first passivated. This was accomplished by annealing 8-arm PEG *via* condensation of the terminal alcohols with the native oxide of silicon using a strategy first reported by Russell and Hawker.[56] The presence of surface-bound PEG was confirmed by an increase in advancing contact angle measurement from 9 ± 3° for freshly cleaned silicon wafers to 32 ± 1° for wafers with annealed PEG. The later measurement is similar to known values for SAMs of PEG on silicon substrates.[26,57,58] Further evidence for PEG immobilization was found in the elemental composition of the surface by energy dispersive X-ray analysis (Table S1). Carbon and oxygen content in the analyzed volume of the surface increased from 37% to 52%, and from 17% to 25%, respectively, following PEG annealing; whereas silicon content dropped from 45% to 22%.

E-beam lithography was then used to fabricate micropatterns composed of a 1:1 blend of PEG-AO and pSS-*co*-PEGMA. PEG-AO was prepared by Mitsunobu coupling of *N*-hydroxyphthalimide to 8-arm hydroxyl-terminated PEG (MW = 20 kDa) followed by hydrazine deprotection. This resulted in installation of aminooxy groups at 97% of the PEG termini by ^{1}H NMR. pSS-*co*-PEGMA was synthesized by reversible addition−fragmentation chain transfer copolymerization of sodium 4-styrenesulfonate and poly(ethylene glycol methacrylate) with AIBN in the presence of *S*-thiobenzoyl-2-thiopropionate. The resulting copolymer had a molecular weight of 24 kDa, a SS:PEGMA ratio of 2.2:1, and a polydispersity index of 1.17 by gel permeation chromatography.

The patterns fabricated from these polymers were designed to immobilize ketone-modified GRGDSPG via oxime bond formation[52,53] with the *O*-hydroxylamines and bFGF by affinity interaction with the sulfonate groups[54,55] as illustrated in Scheme 1. Prior to cell adhesion experiments, cross-linking and biomolecule patterning were verified. Test wafers were patterned with 5 μm circles by e-beam lithography. The 5 μm feature size was chosen for ease of visualization in the fluorescence microscope. Both height (Figure 1a) and phase (Figure 1b) images obtained by AFM showed features that were uniform across the top, suggesting no phase segregation. Furthermore, no evidence of phase segregation was observed in AFM images with a resolution of 2 nm. Images taken in water showed uniform swelling, as well as uniform friction, across the top of the features (Figure S1).

The Lev-RGDSPG-OH was prepared by solid-phase synthesis and conjugated to the surface by simple incubation in slightly acidic buffer. Oxime bond formation leads to chemoselective reaction of biomolecules and has previously been employed for immobilization of keto-functionalized proteins and peptides on e-beam-patterned PEG-AO hydrogels.[49,50] bFGF was immobilized on the heparin-mimicking polymer, pSS-*co*-PEGMA. Heparan sulfate is an ECM component that acts as a depot for bFGF and protects it from denaturation *in vivo*.[17−19] We have previously reported that pSS-*co*-PEGMA is a heparin mimic and can be used to immobilize bFGF on surfaces.[48]

The presence of RGD on the patterns was verified by sequential incubation of the surfaces with soluble human integrin, antihuman integrin, and an AlexaFluor 488-labeled secondary antibody (Figure 1c). Immobilization of bFGF on patterns was verified by sequential incubation with anti-bFGF and an AlexaFluor 568-labeled secondary antibody (Figure 1d). In both cases, fluorescence was observed (green and red, respectively) as expected. Overlay of images from immunostaining for each component confirmed the colocalization of both RGD and bFGF on the features (Figure 1e). The use of a heparin-mimicking polymer to immobilize bFGF is significant as it can present the growth factor in a manner more similar to the natural ECM, where it binds to the proteoglycan heparan sulfate. Staining of bFGF indicated that the surface bound growth factor was immunochemically active; we have found the bFGF antibody does not bind to the denatured growth factor (Figure S2). The bFGF remained active on the surface after longer incubation (4 days) in media as indicated by similar intensity of immunostaining for surface-bound bFGF (Figure S2). This demonstrates the ability of the polymer to stabilize the factor for cell culture; this is critical for this protein, which is easily denatured. It also shows that the protein binds to the polymer in cell culture media.

Cell adhesion on artificial ECM surfaces was investigated with HUVECs, which express both integrins for fibronectin-derivatized RGD and high-affinity FGF receptors (FGFRs). It has been demonstrated that both human fibronectin and FGF are essential for HUVEC proliferation, migration, and survival.[59−62] First, cell adhesion on surfaces containing both RGD and bFGF were studied. HUVECs were cultured on 1 × 1 mm patterns composed of 1 μm squares with a center-to-center spacing of 3 μm for four days to allow focal adhesions to fully develop.[63] This feature size was chosen as it has been

dx.doi.org/10.1021/ja205524x | *J. Am. Chem.Soc.* 2012, 134, 247−255

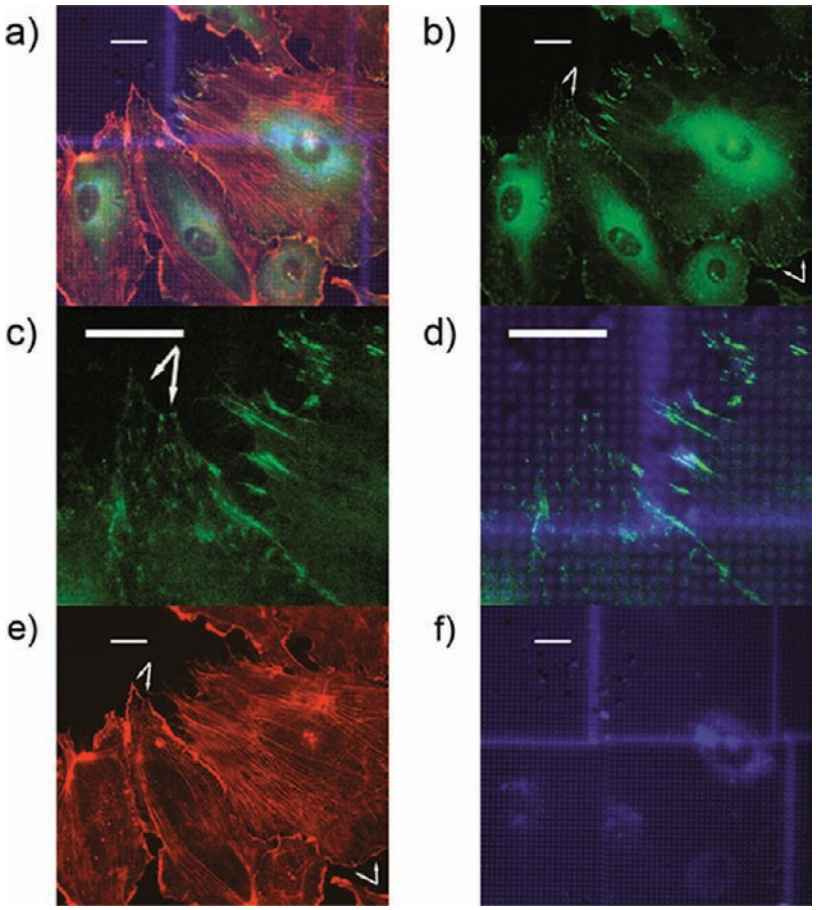

Figure 2. Fluorescence images of HUVECs adhered on ECM-mimicking substrate containing both RGD and bFGF. (a) Actin filaments (red) terminating at focal adhesions (green) are visible in the composite image. (b) Focal adhesions are more clearly visible in the single-channel image corresponding to vinculin staining, and in the zoomed image (c), and are highlighted with white arrows. The focal adhesions are colocalized with the ECM features (d). A square arrangement of actin filaments termini was also observed as illustrated by the white arrows (e), with spacing identical to that of the underlying pattern (f). Scale bars = 20 μm.

reported as the minimum characteristic dimension of focal complexes,[4] and smaller features, depending on the spacing, are known to support focal adhesion formation.[38] While e-beam lithography is a serial technique, which can be slow, the total patterning time for each substrate was 5 min. The cells and patterns were visualized by fluorescence microscopy as shown in Figure 2.

Vinculin is one of the most abundant focal adhesion proteins, which is known to mediate the interaction between actin and the cytoplasmic domain of integrins, and its staining has been utilized as an indicator of focal adhesion formation.[64] Immunostaining of investigated cells, shown in Figure 2b, showed that antivinculin was present throughout the cytoplasm (visible as a green background inside the cell) and was enriched at punctated dots, suggesting focal adhesions. The actin stress fibers were spread throughout the cell (Figure 2e), with termini clustered at the vinculin-rich sites, indicated by the intensified red fluorescence at green-fluorescent dots, confirming the recruitment of actin filaments to the integrin domain of the plasma membrane, i.e. the formation of focal adhesion assemblies.[65] It is notable that focal adhesions were colocalized with the ECM-mimetic features which were stained blue using coumarin in the fluorescence images (Figure 2d), suggesting that cells were forming focal adhesions at the areas engineered with artificial dual ECM components. HUVECs were also well spread on these substrates, with an average area of 6900 ± 100 μm^2.

In order to examine the effect of each ligand alone, experiments were performed using substrates functionalized with only RGD or only bFGF. Figure 3 depicts fluorescent images of the cells cultured on substrates incorporating only RGD as an adhesion component. As expected, HUVECs adhered to these substrates. Focal adhesions were observed by both vinculin staining, and by the intensity of actin filaments on top of the patterned features. The HUVECs were spread on the surface, with an average area of 3000 ± 1000 μm^2. On the substrates incorporating only bFGF, a few HUVECs were attached to the patterned area as shown in Figure 4a. As expected, clear focal adhesions were not observed in the absence of RGD. The cells also did not appear to be as visibly spread on the surface when only bFGF was presented. Indeed, the average area covered by cells cultured on the bFGF alone substrates was only 1200 ± 300 μm^2.

Control experiments were also conducted. Figure S3a shows the adhesion on a double-negative control substrate, which contained neither RGD nor bFGF. As expected, cell adhesion was not observed: a single cell was found, and was neither spread nor intact, further corroborating that the cell adhesion observed in Figure 4a was indeed mediated by bFGF and not the polymer scaffold itself. This result also demonstrates that both the PEG background and the sulfonate- and aminooxy-

dx.doi.org/10.1021/ja205524x | J. Am. Chem.Soc. 2012, 134, 247−255

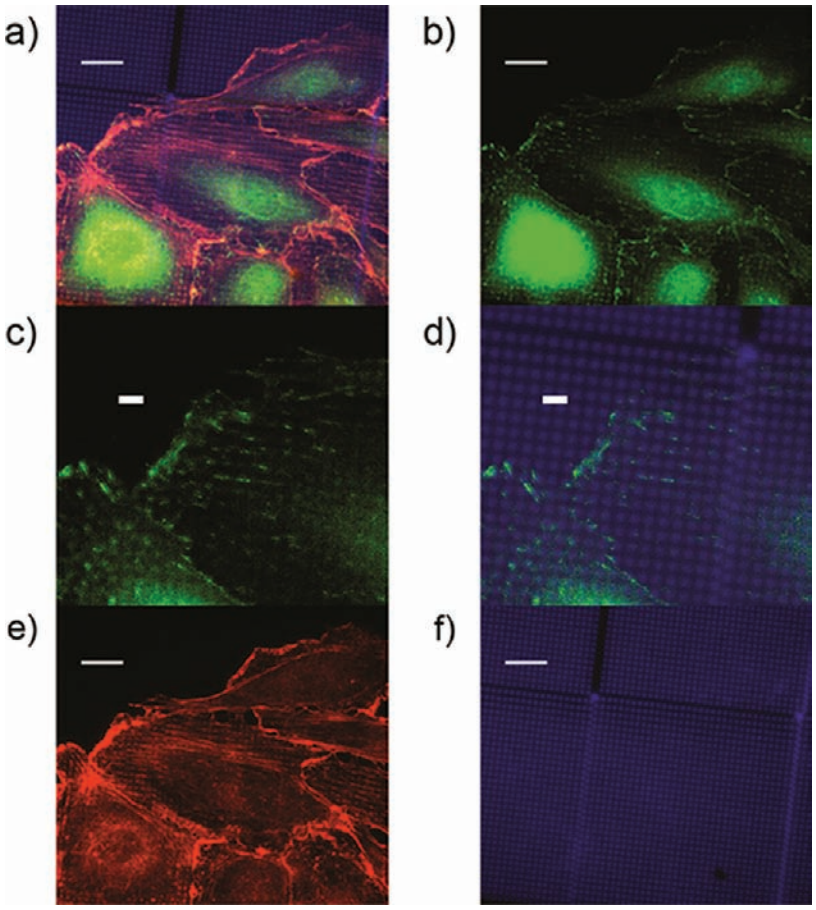

Figure 3. Fluorescence images of HUVECs adhered on RGD-functionalized patterns in the absence of bFGF. (a) Composite image showing actin filaments (red), focal adhesions (green) and the underlying pattern (blue). (b) Single-channel image showing vinculin staining, which are more clearly visible in the zoomed image shown in (c). The punctated dots of vinculin are colocalized with the ECM features in (d). (e) Single-channel image showing actin staining. (f) Single-channel image showing the underlying pattern. Scale bars = 20 μm.

functionalized PEG hydrogel features were cell resistant. Cells could not bind without the signaling molecules present, and HUVEC were not able to deposit their own ECM components on either the PEG hydrogels or background. As an additional control, HUVECs were cultured on fully functionalized substrates with soluble RGDSL present in the cell culture medium at a sufficient concentration to inhibit adhesion *via* integrin binding.[66] Adherent HUVECs were not observed when 2.0 mM RGD peptide was added to the culture medium (Figure S3b). This suggests that the soluble RGD competitively bound to integrins $\alpha_V\beta_3$ and $\alpha_V\beta_5$, thus preventing the formation of focal adhesions with the substrate. Saturation of RGD-interacting integrins resulted in the inhibition of cell attachment to the substrate, which is an important initial stage of focal adhesion formation.[67] This shows that adhesion of HUVEC to these surfaces is mediated by integrin binding.

The data together demonstrate that HUVECs adhere to e-beam-patterned PEG hydrogels. Cells cultured on substrates that present both RGD and bFGF and RGD alone were spread on the surface and displayed many focal adhesions when stained for vinculin. Without RGD or with competitive RGD, cells did not bind. Thus, consistent with literature reports; RGD was required for robust cell adhesion. bFGF alone did promote weak adhesion independent of RGD; however only a few cells were adhered and were not significantly spread (Figure 5). Integrin and growth factor receptor share signaling pathways within the focal adhesion complex,[23] and this could explain why some HUVECs did adhere to substrates presenting only bFGF.

Quantification of cell area showed statistically larger cell areas when bFGF was present with RGD compared to RGD alone (Figure 5). It has been demonstrated that growth factors coordinate integrin signaling.[6] There have been reports that treatment with bFGF improves the expression of $\alpha_V\beta_3$,[21] enhancing cell adhesion, motility, and proliferation.[22] Other studies have shown that osteoblast, primary nerve, and neuronal stem cell adhesion are enhanced on RGD when bFGF is added to the culture medium.[24,68] Our results are consistent with these reports. In addition, protrusions were visible in the images of cells cultured on substrates that present both RGD and bFGF. This is consistent with the role of bFGF in promoting cell migration. While conclusions about enhancement of cell adhesion on the surfaces are difficult to make from cell area alone, the results do suggest that cellular response is improved on surfaces containing bFGF. This corroborates the immunostaining data and indicates that the bFGF remains active on the pSS-*co*-PEGMA. Studies to further elucidate the biological activity of the surface-bound bFGF on HUVECs cultured on these surfaces and verification of the biological pathways are underway. In addition, these surfaces should be excellent model substrates to further understand the synergistic effect of bFGF with integrin ligands in general.

Unlike heparin that can be broken down by heparinases, pSS-*co*-PEGMA is not likely altered by cells to release bFGF for cell

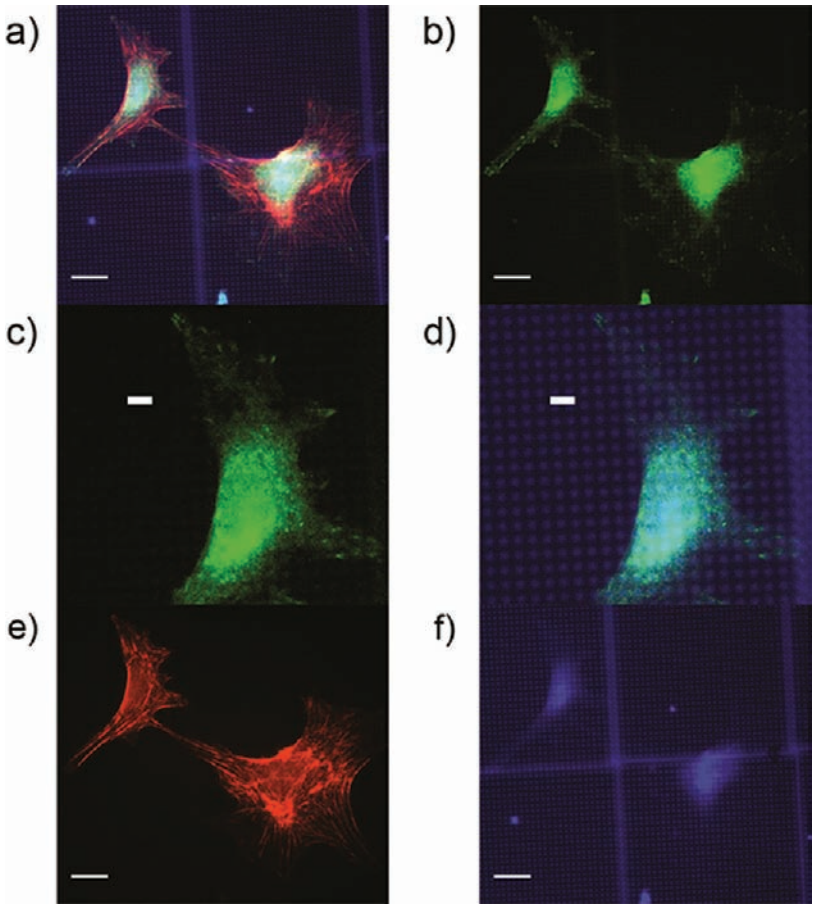

Figure 4. Fluorescence images of HUVECs adhered on bFGF-functionalized patterns in the absence of RGD. (a) Composite image showing actin filaments (red), vinculin (green), and the underlying pattern (blue). (b) Single-channel image showing vinculin staining, with zoomed image shown in (c) and zoomed overlay with underlying surface (d). (e) Single-channel image showing actin staining. (f) Single-channel image showing the underlying pattern. Scale bars = 20 μm.

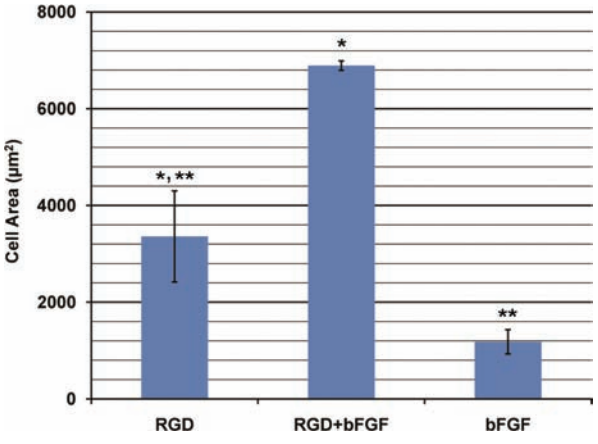

Figure 5. Cell areas on different substrates. HUVEC cultured on substrates presenting both RGD and bFGF spread over a significantly larger area than HUVEC cultured on substrates presenting either ECM component alone. Cells cultured on substrates presenting only RGD were also highly spread, while cells cultured on substrates presenting only bFGF were not. * indicates results significantly different from RGD (p = 0.009). ** indicates results significantly different from RGD (p = 0.04).

binding and internalization. Bovine capillary endothelial cells were found to release heparin-like molecules that liberated matrix-bound bFGF, which could be a mode of release from the pSS-*co*-PEGMA.[69] However, recently for a related growth factor, vascular endothelial growth factor (VEGF), release of the protein from surfaces was found to not be required for signaling in HUVEC cells.[70] In addition, the signaling and resultant cell morphologies stimulated by soluble VEGF versus surface bound protein were different.[71,72] Therefore, the model substrates described here will be useful to study signaling pathways of surface bound factor and/or mode of release of bFGF from the sulfonated polymer.

Quantification of focal adhesions was also carried out. The punctated dots observed in the fluorescence images corresponding to vinculin staining were counted and normalized to the measurement area. Interestingly, the focal adhesion densities measured in HUVEC cultured on all RGD and RGD plus bFGF substrates were identical; an average of 39 focal adhesions were found in every 1000 μm^2. This is lower than the density of ECM-mimetic features (1000 μm^2); some visible focal adhesions appear to span areas larger than one feature size, which could partly explain the differences observed. The result does indicate that the focal adhesion density of cells cultured on these engineered surfaces is controlled by the underlying substrate.

The method described herein provides access to patterns that present both an integrin ligand and growth factor to promote cell adhesion. Although, bFGF was the focus of this paper, the pSS-*co*-PEGMA polymer binds to other heparin-mimicking growth factors such as VEGF,[48] and this same strategy should

enable incorporation of VEGF with integrin ligands. In addition, we demonstrated micron-sized features of the same shape. However, e-beam lithography allows for arbitrary shape formation and nanosized features.[45−49] Thus, myriad geometries at the nanoscale may be envisioned allowing one to study the effect of shape and size on subcellular signaling. These are just some of the many potential applications enabled by this fabrication strategy.

CONCLUSIONS

The ECM is a complex integrated system that provides cellular support and transmits signaling cues. We have successfully demonstrated the production of a surface, which presents both cell-adhesion factors and growth factors at subcellular-length scales. This was accomplished by first fabricating PEG hydrogel features with aminooxy groups and styrene sulfonate using e-beam lithography. HUVECs not only adhered and spread but also formed focal adhesion assemblies in the presence of both components. We have demonstrated that bFGF remained active on the heparin-mimic polymer in culture media, and results suggest that cellular response to the surface was improved by the presence of the factor. We envision that the platform developed here should be of general interest for diverse applications in biomaterials.[73]

EXPERIMENTAL SECTION

Materials and Methods. Amino acids, coupling reagents, and polymer resin were purchased from EMD Chemicals, Inc. (Germany). bFGF was obtained from the National Cancer Institute. All other chemicals were purchased from Sigma-Aldrich Co. unless otherwise noted. All chemicals were used as received. Gel permeation chromatography (GPC) was conducted on a Shimadzu HPLC system equipped with a refractive index detector RID-10A and two Polymer Laboratories PLgel 5 μm mixed D columns (with guard column) with lithium bromide (0.1 M) in *N*,*N*-dimethylformamide (DMF) as the mobile phase. Near-monodisperse poly(methyl methacrylate) (PMMA) standards (Polymer Laboratories) were employed for calibration. Contact angle goniometry was performed on an FTA 4000 contact angle goniometer (First Ten Angstroms, Portsmouth, VA), and is reported as the average of measurements on three different locations of three chips for each surface. Energy dispersive X-ray analysis was performed on a JEOL JSM-6701F scanning electron microscope equipped with a Sapphire Si(Li) detecting unit (EDAX, Mahwah, NJ). Atomic force microscopy (AFM) images were obtained on a Veeco Dimension 5000 scanning probe microscope in tapping mode equipped with a BS-Tap 300 silicon cantilever (Budget Sensors) at a scan rate of 1 Hz, and a resolution of 512 × 512 pixels.

Synthesis of RGD-Containing Peptides. The RGD-containing peptides were synthesized *via* standard solid-phase peptide synthesis methods, using a 2-chlorotrityl chloride resin and HBTU (*O*-(benzotriazol-1-yl)-*N*,*N*,*N*′,*N*′-tetramethyluronium hexafluorophosphate) as a coupling reagent. A ketone was installed on the *N*-terminus of NH_2-GRGDSPG-OH by HBTU coupling with Fmoc-5-aminolevulinic acid (AnaSpec, Inc., Fremont, CA) on the resin. NH_2-RGDSL-OH was synthesized for the competitive cell binding assay as a control. The peptides were cleaved from the resin and side-chains were deprotected by treatment in trifluoroacetic acid (TFA)/triisopropylsilane (TIS)/water mixture (95:2.5:2.5, v/v/v) at 24 °C for 4 h. The resin was removed by filtration through 0.4 μm PTFE syringe filter, and the solution was precipitated into diethyl ether to give a white solid. Lev-GRGDSPG-OH was further purified by preparative reverse-phase HPLC on a Luna 5 μm C18 column (Phenomenex, Inc., Torrance, CA), under a linear gradient from 95:5 to 5:95 of water/acetonitrile (containing 0.1% of trifluoroacetic acid) at 10 mL/min. The peptide was collected from fractions that eluted between 15 and 17 min. NH_2-RGDSL-OH was used without further purification. The molecular weights of each peptide were verified *via* electrospray ionization mass spectrometry (ESI-MS) (LCQ Deca Ion Trap MS, Thermo Finnigan, Waltham, MA): m/z 758.47 [$(M + H)^+$, calcd 758.34] for the NH_2-Lev-GRGDSPG-OH peptide, and m/z 547.33 [$(M + H)^+$, calcd 547.58] for the NH_2-RGDSL-OH peptide. The mass spectra are provided in the Supporting Information (Figure S4).

Synthesis of Aminooxy-Terminated 8-arm PEG (PEG-AO). PEG-AO was synthesized as previously described.[49]

Synthesis of Poly(styrene-4-sulfonate-co-poly(ethylene glycol)methacrylate) (pSS-co-PEGMA). pSS-*co*-PEGMA was synthesized as previously described.[48]

Micropatterning of Surface via E-beam Lithography. Silicon wafers (SQI International) were cleaned for 10 min in freshly prepared piranha solution (**CAUTION**: piranha solution reacts violently with organics and must be handled with care!) and rinsed with Milli-Q water. The wafers were then spin-coated with a 1% w/v solution of 8-arm PEG (MW = 20,000, Nektar) in methanol at 3000 rpm for 30 s, and baked at 120 °C for 10 min to anneal the PEG to the native oxide layer. The excess PEG was rinsed off with Milli-Q water. The PEG-coated wafer was spin-coated at 3000 rpm for 30 s with a solution of 0.5% w/v 8-arm aminooxy-terminated PEG and 0.5% w/v pSS-*co*-PEGMA in methanol. The wafers were then patterned with a JEOL 5910 scanning electron beam microscope. Pattern files for 1 × 1 μm features in a square array with 3 μm center-to-center spacing were created in DesignCAD 2000 and written with a JC Nabity lithography system (Nanometer Pattern Generation System, ver. 9.0). Patterns were exposed using an area dose of 150 μC/cm^2. After exposure, uncross-linked polymer was rinsed away with Milli-Q water. Patterning was confirmed by AFM.

Immobilization of ECM Components. The cell adhesion domain (RGD) was introduced on the aminooxy-patterned surface by incubating with Lev-GRGDSPG-OH peptide (100 μg/mL, PBS, pH 5.5) at 23 °C for 18 h. (All experiments hereafter were performed in the dark until the image analysis in order to avoid photoquenching.) Each surface was then rinsed with Milli-Q water and incubated with 2 mg/mL maleimido coumarin (7-diethylamino-3-(4′-maleimidyl-phenyl)-4-methylcoumarin, Invitrogen, Carlsbad, CA) in dimethyl sulfoxide (DMSO), at 23 °C for 1 h, to bind to remaining aminooxy groups and allow visualization of patterns on the surface. After rinsing with DMSO (3×), the surfaces were sterilized in 70% isopropyl alcohol at 23 °C for 15 min and washed with Dulbecco's PBS (D-PBS) (3×). Each surface was then incubated with 100 μg/mL bFGF (recombinant human FGF basic, R&D Systems, Inc., Minneapolis, MN) at 4 °C for 1 h. The surfaces were then washed with cell culture medium prior to cell seeding. Surfaces with RGD only, bFGF only, and without RGD or bFGF were also prepared by omitting certain incubations, respectively, as controls. RGD and bFGF immobilization were confirmed by immunostaining. Test substrates were incubated with human integrin $\alpha_V\beta_5$ (32.5 μg/mL in D-PBS, Chemicon International, Temecula, CA) for 1 h, then a mixture of mouse antihuman integrin $\alpha_V\beta_5$ IgG (1 mg/mL in D-PBS, Invitrogen) and sheep anti-bFGF IgG (1:1000 dilution in D-PBS, Chemicon International) for 1 h, and finally a mixture of AlexaFluor 488 antimouse IgG (20 μg/mL in D-PBS, Invitrogen) and AlexaFluor 568 goat antisheep IgG (10 μg/mL, Invitrogen) for 30 min. Substrates were rinsed with D-PBS following each incubation step.

Cell Adhesion Study. Cell adhesion studies on the patterned surfaces were performed with HUVECs (PromoCell GmbH, Heidelberg, Germany). All cell culture experiments were carried out at 37 °C in a 5% CO_2 atmosphere using 2% fetal calf serum-containing endothelial cell growth medium (PromoCell GmbH) as recommended by the supplier, except that the bFGF supplement was not added to the media when incubated with the patterned surfaces. Cells between passages 3 and 7 were used. On each patterned surface cells were seeded with an initial density of 1000 cells per well, which contained a single wafer (typical concentration of cells in the seeding solution was 200 per 1 μL), in a 6-well plate. After allowing the cells to settle for 15 min, medium was added and the cells were incubated for 4 days. Negative control experiments were carried out by seeding cells on patterned surfaces in the absence of one or more ECM component

(with no ligands, with RGD only, and with bFGF only). A competitive binding assay, as a stringent control, was performed on the RGD-immobilized surface by adding NH_2-RGDSL-OH (2 mM as a soluble form) in the initial cell seeding. All experiments were performed with at least six replicates.

Staining and Image Analysis with Fluorescence Microscopy. The surfaces incubated with cells were washed with fresh endothelial cell growth medium. Cells were then fixed in 4% paraformaldehyde (in D-PBS) at 23 °C for 15 min, and permeabilized by washing with 0.05% Triton X-100. Each surface was incubated in 1% bovine serum albumin (BSA, in D-PBS) at 23 °C for 30 min, followed by FITC-antivinculin (20 μg/mL in 1% BSA, Sigma, St. Louis, MO) at 37 °C for 2 h to visualize the focal adhesions. To visualize the cell spreading, filamentous actin was stained with AlexaFluor 568-conjugated phalloidin (~63 ng/mL, Invitrogen) at 23 °C for 30 min. Between each step, the surfaces were carefully washed with D-PBS (5 times, 5 min each wash). The wafers were mounted on a glass slide using Fluoro-gel mounting medium (Electron Microscopy Sciences Co., Hatfield, PA), and sealed using clear nail polish. Images of stained samples were acquired on an AxioCam MRm camera mounted on an Axiovert 200 inverted microscope equipped with a FluoArc mercury lamp (Carl Zeiss MicroImaging GmbH, Germany), using Axio Vision 4.8 software. Cell areas were quantified in a blinded study by measuring the outline of AlexaFluor 568 fluorescence from adhered cells. Statistical comparisons between each data set were performed on Microsoft Excel using a two-sided *t* test. Focal adhesion density was quantified from AlexaFluor 488 fluorescence using Imaris 7.2.3 software (Bitplane AG, Zürich, Switzerland) by counting the number of surfaces exceeding a threshold of 30 counts relative to local background.

■ ASSOCIATED CONTENT

Ⓢ Supporting Information

EDAX analysis of patterned substrates, characterization data for peptides, control images, and detailed AFM images of test wafers.This material is available free of charge via the Internet at http://pubs.acs.org.

■ AUTHOR INFORMATION

Corresponding Author

maynard@chem.ucla.edu

Present Address

‡Department of Chemistry, University of Southern California, 3620 McClintock Avenue, Los Angeles, CA 90089-1062, United States.

■ ACKNOWLEDGMENTS

This research was funding by the National Science Foundation Career Award (CHE-0645793) and the Center for Scalable and Integrated NanoManufacturing (SINAM, DMI-0327077). C.M.K. acknowledges a fellowship from the NSF IGERT: Materials Creation Training Program (MCTP)-DGE-0654431 and the California NanoSystems Institute. H.D.M. acknowledges the Alfred P. Sloan Foundation for additional funding. S.S.S. thanks the Swiss National Science Foundation for the Fellowship (PBEZP2- 133211). We thank the National Cancer Institute for providing bFGF. We thank Thi Nguyen for performing blinded quantification studies and for helpful discussions. We acknowledge the use of the Scanning Probe Microscopy facility at the Nano and Pico Characterization Laboratory at the California NanoSystems Institute.

■ REFERENCES

(1) Jung, D. R.; Kapur, R.; Adams, T.; Giuliano, K. A.; Mrksich, M.; Craighead, H. G.; Taylor, D. L. *Crit. Rev. Biotechnol.* **2001**, *21*, 111–154.
(2) Falconnet, D.; Csucs, G.; Grandin, H. M.; Textor, M. *Biomaterials* **2006**, *27*, 3044–3063.
(3) Rosso, F.; Giordano, A.; Barbarisi, M.; Barbarisi, A. *J. Cell. Physiol.* **2004**, *199*, 174–180.
(4) Geiger, B.; Bershadsky, A.; Pankov, R.; Yamada, K. M. *Nat. Rev. Mol. Cell Biol.* **2001**, *2*, 793–805.
(5) Tamkun, J. W.; Desimone, D. W.; Fonda, D.; Patel, R. S.; Buck, C.; Horwitz, A. F.; Hynes, R. O. *Cell* **1986**, *46*, 271–282.
(6) Mark, K.; Schöber, S.; Goodman, S. L. In *Integrin Protocols*; Howlett, A., Ed.; Humana Press: Totowa, NJ, 1999; p 219–230.
(7) Wu, J. M.; Rosser, M. P.; Howlett, A. R.; Feldman, R. I. In *Integrin Protocols*; Howlett, A., Ed.; Humana Press: Totowa, NJ, 1999; pp 211–217.
(8) Pierschbacher, M. D.; Ruoslahti, E. *Nature* **1984**, *309*, 30–33.
(9) Ruoslahti, E.; Pierschbacher, M. D. *Science* **1987**, *238*, 491–497.
(10) Brooks, P. C.; Montgomery, A. M. P.; Rosenfeld, M.; Reisfeld, R. A.; Hu, T.; Klier, G.; Cheresh, D. A. *Cell* **1994**, *79*, 1157–1164.
(11) Hammes, H.-P.; Brownlee, M.; Jonczyk, A.; Sutter, A.; Preissner, K. T. *Nat. Med.* **1996**, *2*, 529–533.
(12) Horton, M. A.; Dorey, E. L.; Nesbitt, S. A.; Samanen, J.; Ali, F. E.; Stadel, J. M.; Nichols, A.; Greig, R.; Helfrich, M. H. *J. Bone Miner. Res.* **1993**, *8*, 239–247.
(13) Medhora, M. M.; Teitelbaum, S.; Chappel, J.; Alvarez, J.; Mimura, H.; Ross, F. P.; Hruska, K. *J. Biol. Chem.* **1993**, *268*, 1456–1461.
(14) Nip, J.; Brodt, P. *Cancer Metastasis Rev.* **1995**, *14*, 241–252.
(15) Turner, N.; Grose, R. *Nat. Rev. Cancer* **2010**, *10*, 116–129.
(16) Hunger-Glaser, I.; Fan, R. S.; Perez-Salazar, E.; Rozengurt, E. *J. Cell. Physiol.* **2004**, *200*, 213–222.
(17) Taipale, J.; Keski-Oja, J. *FASEB J.* **1997**, *11*, 51–59.
(18) Elcin, Y. M.; Dixit, V.; Gitnick, T. *Artif. Organs* **2001**, *25*, 558–565.
(19) Galzie, Z.; Fernig, D. G.; Smith, J. A.; Poston, G. J.; Kinsella, A. R. *Int. J. Cancer* **1997**, *71*, 390–395.
(20) Eliceiri, B. P.; Cheresh, D. A. *Curr. Opin. Cell Biol.* **2001**, *13*, 563–568.
(21) Brooks, P. C.; Clark, R. A.; Cheresh, D. A. *Science* **1994**, *264*, 569–571.
(22) Ingber, D. E.; Prusty, D.; Frangioni, J. V.; Cragoe, E. J.; Lechene, C.; Schwartz, M. A. *J. Cell Biol.* **1990**, *110*, 1803–1811.
(23) Plopper, G. E.; McNamee, H. P.; Dike, L. E.; Bojanowski, K.; Ingber, D. E. *Mol. Biol. Cell* **1995**, *6*, 1349–1365.
(24) Freudenberg, U.; Hermann, A.; Welzel, P. B.; Stirl, K.; Schwarz, S. C.; Grimmer, M.; Zieris, A.; Panyanuwat, W.; Zschoche, S.; Meinhold, D.; Storch, A.; Werner, C. *Biomaterials* **2009**, *30*, 5049–5060.
(25) Nie, T.; Akins, R. E. Jr; Kiick, K. L. *Acta Biomater.* **2009**, *5*, 865–875.
(26) Sorribas, H.; Padeste, C.; Tiefenauer, L. *Biomaterials* **2002**, *23*, 893–900.
(27) Mrksich, M. *Acta Biomater.* **2009**, *5*, 832–41.
(28) Massia, S. P.; Hubbell, J. A. *J. Cell Biol.* **1991**, *114*, 1089–1100.
(29) Roberts, C.; Chen, C. S.; Mrksich, M.; Martichonok, V.; Ingber, D. E.; Whitesides, G. M. *J. Am. Chem. Soc.* **1998**, *120*, 6548–6555.
(30) Chen, C. S.; Mrksich, M.; Huang, S.; Whitesides, G. M.; Ingber, D. E. *Science* **1997**, *276*, 1425–8.
(31) McBeath, R.; Pirone, D. M.; Nelson, C. M.; Bhadriraju, K.; Chen, C. S. *Dev. Cell* **2004**, *6*, 483–95.
(32) Luo, W.; Jones, S. R.; Yousaf, M. N. *Langmuir* **2008**, *24*, 12129–33.
(33) Chan, E. W.; Yousaf, M. N. *Mol. BioSyst.* **2008**, *4*, 746–53.
(34) Park, S.; Yousaf, M. N. *Langmuir* **2008**, *24*, 6201–7.
(35) Senaratne, W.; Sengupta, P.; Jakubek, V.; Holowka, D.; Ober, C. K.; Baird, B. *J. Am. Chem. Soc.* **2006**, *128*, 5594–5595.

(36) Lee, K. B.; Park, S. J.; Mirkin, C. A.; Smith, J. C.; Mrksich, M. *Science* **2002**, *295*, 1702−1705.
(37) Hoover, D. K.; Chan, E. W. L.; Yousaf, M. N. *J. Am. Chem. Soc.* **2008**, *130*, 3280−3281.
(38) Arnold, M.; Cavalcanti-Adam, E. A.; Glass, R.; Blummel, J.; Eck, W.; Kantlehner, M.; Kessler, H.; Spatz, J. P. *ChemPhysChem* **2004**, *5*, 383−388.
(39) Arnold, M.; Schwieder, M.; Blummel, J.; Cavalcanti-Adam, E. A.; Lopez-Garcia, M.; Kessler, H.; Geiger, B.; Spatz, J. P. *Soft Matter* **2009**, *5*, 72−77.
(40) Schlenoff, J. B.; Li, M.; Ly, H. *J. Am. Chem. Soc.* **1995**, *117*, 12528−12536.
(41) Flynn, N. T.; Tran, T. N. T.; Cima, M. J.; Langer, R. *Langmuir* **2003**, *19*, 10909−10915.
(42) King, P. A.; Ward, J. A. *J. Polym. Sci., Part A: Polym. Chem.* **1970**, *8*, 253−262.
(43) Zhang, L.; Zhang, W.; Zhang, Z.; Yu, L.; Zhang, H.; Qi, Y.; Chen, D. *Int. J. Radiat. Appl. Instrum. C Radiat. Phys. Chem.* **1992**, *40*, 501−505.
(44) Krsko, P.; Sukhishvili, S.; Mansfield, M.; Clancy, R.; Libera, M. *Langmuir* **2003**, *19*, 5618−5625.
(45) Hong, Y.; Krsko, P.; Libera, M. *Langmuir* **2004**, *20*, 11123−11126.
(46) Brough, B.; Christman, K. L.; Wong, T. S.; Kolodziej, C. M.; Forbes, J. G.; Wang, K.; Maynard, H. D.; Ho, C. M. *Soft Matter* **2007**, *3*, 541−546.
(47) Saaem, I.; Papasotiropoulos, V.; Wang, T.; Soteropoulos, P.; Libera, M. *J. Nanosci. Nanotechnol.* **2007**, *7*, 2623−2632.
(48) Christman, K. L.; Vazquez-Dorbatt, V.; Schopf, E.; Kolodziej, C. M.; Li, R. C.; Broyer, R. M.; Chen, Y.; Maynard, H. D. *J. Am. Chem. Soc.* **2008**, *130*, 16585−16591.
(49) Christman, K. L.; Schopf, E.; Broyer, R. M.; Li, R. C.; Chen, Y.; Maynard, H. D. *J. Am. Chem. Soc.* **2009**, *131*, 521−527.
(50) Kolodziej, C. M.; Chang, C.-W.; Maynard, H. D. *J. Mater. Chem.* **2011**, *21*, 1457−1461.
(51) Krsko, P.; McCann, T. E.; Thach, T. T.; Laabs, T. L.; Geller, H. M.; Libera, M. R. *Biomaterials* **2009**, *30*, 721−729.
(52) Lemieux, G. A.; Bertozzi, C. R. *Trends Biotechnol.* **1998**, *16*, 506−513.
(53) Maynard, H. D.; Broyer, R. M.; Kolodziej, C. M. In *Click Chemistry for Biotechnology and Materials Science*; Lahann, J., Ed.; John Wiley & Sons, Ltd.: Singapore, 2009; pp 53−68.
(54) Liekens, S.; Neyts, J.; Degreve, B.; DeClercq, E. *Oncol. Res.* **1997**, *9*, 173−181.
(55) Liekens, S.; Leali, D.; Neyts, J.; Esnouf, R.; Rusnati, M.; Dell'Era, P.; Maudgal, P. C.; De Clercq, E.; Presta, M. *Mol. Pharmacol.* **1999**, *56*, 204−213.
(56) Mansky, P.; Liu, Y.; Huang, E.; Russell, T. P.; Hawker, C. J. *Science* **1997**, *275*, 1458−1460.
(57) Papra, A.; Gadegaard, N.; Larsen, N. B. *Langmuir* **2001**, *17*, 1457−1460.
(58) Janssen, D.; De Palma, R.; Verlaak, S.; Heremans, P.; Dehaen, W. *Thin Solid Films* **2006**, *515*, 1433−1438.
(59) Garfinkel, S.; Hu, X.; Prudovsky, I. A.; McMahon, G. A.; Kapnik, E. M.; McDowell, S. D.; Maciag, T. *J. Cell Biol.* **1996**, *134*, 783−791.
(60) Kinoshita, M.; Shimokado, K. *Arterioscler., Thromb., Vasc. Biol.* **1999**, *19*, 2323−2329.
(61) Maciag, T.; Hoover, G. A.; Stemerman, M. B.; Weinstein, R. *J. Cell Biol.* **1981**, *91*, 420−426.
(62) Thornton, S. C.; Mueller, S. N.; Levine, E. M. *Science* **1983**, *222*, 623−625.
(63) Dalby, M. J.; Yarwood, S. J. In *Adhesion Protein Protocols*; Coutts, A. S., Ed.; Humana Press: Totowa, NJ, 2007; pp 121−134.
(64) Burridge, K.; ChrzanowskaWodnicka, M. *Annu. Rev. Cell Dev. Biol.* **1996**, *12*, 463−518.
(65) Critchley, D. R. *Curr. Opin. Cell Biol.* **2000**, *12*, 133−139.
(66) Liu, J. C.; Heilshorn, S. C.; Tirrell, D. A. *Biomacromolecules* **2004**, *5*, 497−504.
(67) Burridge, K.; Fath, K.; Kelly, T.; Nuckolls, G.; Turner, C. *Annu. Rev. Cell Biol.* **1988**, *4*, 487−525.
(68) Jang, J.-H.; Ku, Y.; Chung, C.-P.; Heo, S.-J. *Biotechnol. Lett.* **2002**, *24*, 1659−1663.
(69) Moscatelli, D. *J. Cell Biol.* **1988**, *107*, 753−759.
(70) Anderson, S. M.; Shergill, B.; Barry, Z. T.; Manousiouthakis, E.; Chen, T. T.; Botvinick, E.; Platt, M. O.; Iruela-Arispe, M. L.; Segura, T. *Integr. Biol.* **2011**, *3*, 887−896.
(71) Chen, T. T.; Luque, A.; Lee, S.; Anderson, S. M.; Segura, T.; Iruela-Arispe, M. L. *J. Cell Biol.* **2010**, *188*, 595−609.
(72) Anderson, S. M.; Chen, T. T.; Iruela-Arispe, M. L.; Segura, T. *Biomaterials* **2009**, *30*, 4618−4628.
(73) Discher, D. E.; Mooney, D. J.; Zandstra, P. W. *Science* **2009**, *324*, 1673−1677.